ACS APPLIED MATERIALS & INTERFACES

Forum Article

www.acsami.org

Nanostructured Biointerfaces: Nanoarchitectonics of Thermoresponsive Polymer Brushes Impact Protein Adsorption and Cell Adhesion

Evmorfia Psarra,[†,‡,§] Ulla König,[†,*,‡] Yuichiro Ueda,[⊥] Cornelia Bellmann,[‡] Andreas Janke,[‡] Eva Bittrich,[‡] Klaus-J. Eichhorn,[‡] and Petra Uhlmann*[,‡]

[‡]Leibniz Institute of Polymer Research Dresden, Hohe Strasse 6, 01069 Dresden, Germany

[§]Faculty of Science, Department of Chemistry, Chair of Physical Chemistry of Polymeric Materials, The Technische Universität Dresden, Bergstrasse 66, 01069 Dresden, Germany

[⊥]Department of Biocompatibility, Institute of Biomaterial Science HZG Teltow, Kantstrasse 55, 14513 Teltow, Germany

ABSTRACT: Controlling the reversibility, quantity, and extent of biomolecule interaction at interfaces has a significant relevance for biomedical and biotechnological applications, because protein adsorption is always the first step when a solid surface gets in contact with a biological fluid. Polymer brushes, composed of end-tethered linear polymers with sufficient grafting density, are very promising to control and alter interactions with biological systems because of their unique structure and distinct collaborative response to environmental changes. We studied protein adsorption and cell adhesion at polymer brush substrates which consisted of poly(*N*-isopropylacrylamide) (PNIPAAm), having a lower critical solution temperature (LCST), to control bioadsorptive processes by changing the environmental temperature. Preparing the PNIPAAm brushes by the "grafting-to"-method two differently synthesized PNIPAAm polymers were used, at which one possessed an additional hydrophobic terminal headgroup. It is known that hydrophobic moieties can influence protein adsorption significantly. The films were comprehensively analyzed by in situ spectroscopic ellipsometry, contact angle measurements, streaming potential, and atomic force microscopy. Our study was mainly focused on the investigation of the fibrinogen (FGN) adsorption responsiveness both on homo polymer PNIPAAm brushes with and without the hydrophobic terminal functionalization, and further on binary brushes made of the polyelectrolyte poly(acrylic acid) (PAA) and one of the prior described two PNIPAAm species. The results show that the terminal hydrophobic modification of PNIPAAm has a considerable impact on wettability, LCST, and morphology of the homo and the binary brush systems, which consequently led to an alteration of FGN adsorption. By using binary PNIPAAm-PAA brushes with different composition it was possible to induce stimuli dependent FGN adsorption with a considerable amplified switching effect by introducing a hydrophobic terminal residue to PNIPAAm. Cell adhesion studies with human mesenchymal stem cells reflected the results of the FGN adsorption.

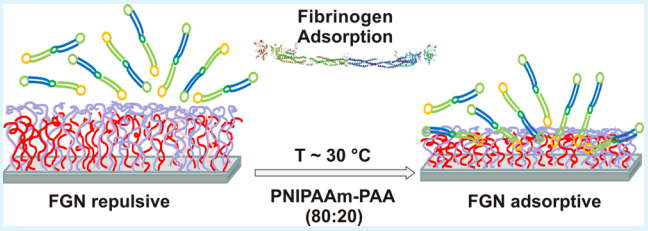

KEYWORDS: *nanomaterials, polymer brush, grafting-to-method, spectroscopic ellipsometry, fibrinogen adsorption, stimuli response*

1. INTRODUCTION

Monitoring of biomolecule interaction and cell adhesion on surfaces is a matter of vast concern for various biotechnological, biomedical, and biomaterial applications. On the one hand, there are several application fields where the prevention of nonspecific protein adsorption and cell adhesion on surfaces is requested. Otherwise, the stimulation of specific biomolecule interaction is a crucial factor for advanced material design developments. Here, smart surfaces that possess reversible properties in response to diverse environmental stimuli are of significance to tailor those interactions.[1,2] In general, the nonspecific affinity of biological species (e.g., proteins/peptides) to interfaces as a well-known phenomenon has to be directed and controlled. In addition to the individual biomolecule attributes, manifold material surface characteristics like topography, chemistry, charge, hydrophilicity/hydrophobicity, or elasticity are relevant determinants for interfacial processes in biological fluids and will be addressed in this article. To control the adsorption characteristics and activity of bound biomolecules, the different features have to act in synergy. Therefore, there is the utmost need to adapt material interfaces to various biotechnological or biomedical applications in consideration of longevity and successful function of materials in biological environments. The advancement of material function and performance is the major issue of surface

Special Issue: Forum on Polymeric Nanostructures: Recent Advances toward Applications

Received: November 20, 2014
Accepted: January 26, 2015
Published: February 4, 2015

DOI: 10.1021/am508161q
ACS Appl. Mater. Interfaces 2015, 7, 12516−12529

engineering aiming the production of tailored materials that specifically control biological responses.[3]

Currently, nanostructured materials are investigated for an enhanced manipulation of these physical, biochemical, and biological issues. This approach has an immense potential for scientific and technological achievements in the field. A special challenge is the medical application of nanotechnology, ranging from implants or drug targeting to nanoelectronic biosensors, because the size of nanomaterials is similar to most of biological species and structures. In this context, the scope of the present paper focuses on bionanotechnological approaches dealing with responsive nanoscaled polymer layers. The benefits of polymer nano coatings, using well-defined, covalently bound, and densely grafted polymer chains have been the subject of many investigations and applications in the fields of material science and bioscience. In particular, polymer brushes, composed of end-tethered linear polymers unidirectionally stretched perpendicularly from the surface due to excluded volume interactions, are very promising to tailor interactions with biological systems due to their unique structure and distinct collaborative response to environmental changes. The covalent binding of preformed, functionalized polymer chains at an interface containing complementary functional groups provokes enhanced stability of the tethered polymer layers and is known as the grafting-to method. It is a technically simple synthesis and the preformed polymers can be precisely characterized before grafting. These advantages make polymer brushes to distinguished surface coatings with novel qualities.[4,5]

In this study, polymer brush surface properties were modulated by changing the chemical composition of the polymer brush layer in order to create appropriate nanostructured biointerfaces. The main driving forces that lead to biomolecular adsorption on any surfaces are hydrophobic and electrostatic interactions, entropic forces and hydrogen bonding. Creating valuable smart materials with adjustable characteristics needs to consider these interactions and to adapt strategies that will help to understand and control them. A very hydrophobic surface is expected to adsorb biomolecules more easily than a less hydrophobic one.[6] In addition, charged materials with ionizable or dissociable groups, such as polyelectrolytes, are expected to attract oppositely charged biomolecules.[7] Our recent research was focused on polymer brush systems with adjustable and alterable characteristics made of stimuli-responsive polymers.

A widely used and fairly characterized, stimuli-responsive polymer is poly(isopropylacrylamide) (PNIPAAm), which undergoes a structural transition in solution when heated above a certain temperature, the lower critical solution temperature (LCST). Dissolved PNIPAAm molecules have the tendency to swell to a full extend for temperatures below 32 °C. When heated above its LCST, PNIPAAm chains collapse and inherit a globular conformation. There are several studies about protein adsorption on PNIPAAm brushes, which generally reveal that PNIPAAm brushes are protein resistant at room temperature, which in some cases might change to protein adsorptive above the LCST.[8,9] Switching at the LCST occurs because of the change in the polymer nature from highly hydrated state to the more hydrophobic, dehydrated conformation. Apart from investigations of protein adsorption on PNIPAAm brushes,[8−11] various other PNIPAAm-based materials such as hydrogels,[12] and PNIPAAm copolymers mixed with additional polymer materials[13] have been studied regarding protein affinity. In addition to the polymer state (hydrogel, brush, etc.), the polymer molecular weight, the brush grafting density, but also the size and nature of the protein under investigation are crucial effecting parameters. In our previous studies, we have shown that PNIPAAm brushes with low grafting densities and molecular weight made by the grafting-to approach are protein repellent above and below the LCST.[9,14] The subject of this study was to investigate how the introduction of a short hydrophobic terminal group into the PNIPAAm chains would influence surface characteristics and interaction potential of the resulting brushes. To the best of our knowledge, biomolecule adsorption on PNIPAAm polymer brushes carrying such a hydrophobic terminal group has not been examined so far. To go one step further into the direction of stimuli-responsive advanced biointerfaces, we investigated protein adsorption on binary poly(isopropylacrylamide)-poly(acrylic acid) (PNIPAAm-PAA) brushes. Weak polyelectrolytes (PE), such as PAA, show a dissociation dependence on the pH value of the solution. The swollen brush thickness is a result of the osmotic pressure inside the brush and the configurational elasticity of the polymeric chains. Protein adsorption at PE brushes is driven by electrostatic interactions and depends on the ionic strength and pH of the surrounding solution as well as the isoelectric point (IEP) of the protein. PAA is increasingly negatively charged above pH 2.1 (IEP_{PAA} in solution), due to dissociation of the carboxylic groups to carboxylates (COOH to COO^-). In the pH region IEP_{PAA} <pH < $IEP_{protein}$, the protein has a positive overall charge, the electrostatic attraction to the surface is strong and therefore, high adsorption is expected. The maximum adsorption normally occurs at a pH value close to the $IEP_{protein}$ where amphiphilic interactions govern, whereas at the "wrong site" above the $IEP_{protein}$, where the surface and protein have the same interfacial charges, minimal but not negligible protein adsorption is expected to occur.[15] The combination of PAA with PNIPAAm to a PNIPAAm-PAA temperature-responsive binary brush should allow for controlling protein adsorption on interfaces in a stimuli responsive manner. We investigated the adsorption of fibrinogen (FGN) glycoprotein as a model protein on polymer brushes to prove this behavior. Fibrinogen is a highly abundant blood plasma glycoprotein synthesized in the liver by hepatocytes having a molecular weight of 340 kDa, and an $IEP_{protein}$ = 5.5.[16] FGN has an elongated conformation, particularly interesting for surface studies that relate to bioapplications. In general, as most of protein molecules, FGN has the tendency to adsorb on flat surfaces, whereas the rate and magnitude of adsorption depends on various parameters such as the nature of the surface and the surrounding media. PNIPAAm has extensively been used as protein repellent coating in various forms, inducing low affinity to certain cell lines.[17] According to investigations of FGN adsorption on end tethered PNIPAAm brushes, prepared by ATRP grafting-from, the brush surface with 13.4 nm dry thickness conserved the protein resistant character above LCST, whereas for thicker dry PNIPAAm brushes of 38.1 nm, a significant increase in FGN adsorption at 37 °C was found.[18]

We focused our investigations on the regulation and control of FGN−surface affinity by modulating hydrophobic interactions due to temperature changes and introduction of an additional subnanometer sized hydrophobic domain in the brush system. The development of a sophisticated nanostructured surface coating that would retain its overall hydrophilicity and under certain conditions enable stimuli

DOI: 10.1021/am508161q
ACS Appl. Mater. Interfaces 2015, 7, 12516−12529

Scheme 1. Illustration of the Scope of This Paper: (A–D) Stepwise Explanation of the Grafting-to Method for the Preparation of the Binary Brush System PNIPAAm-PAA Using Two Different PNIPAAm Species; (E) Subsequent Investigation of the Stimuli Sensitive Fibrinogen Adsorption onto All Homo- And Binary Polymer Brush Compositions

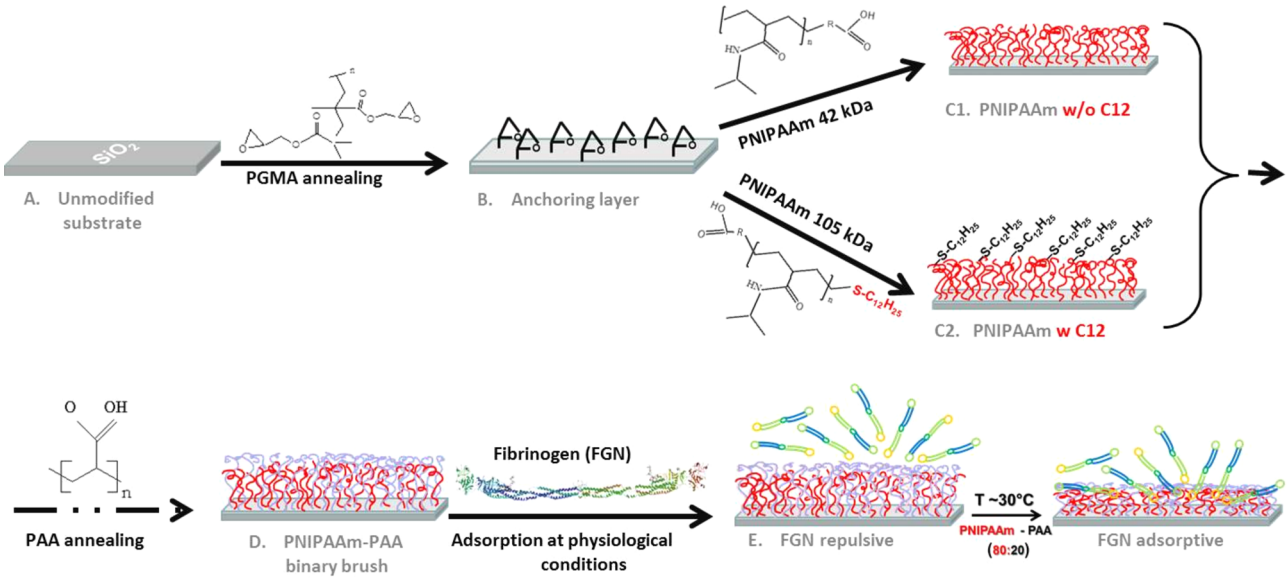

Table 1. Properties of the Applied PNIPAAm Homopolymer Brushes

homobrushes	characteristics	M_n (g/mol)	PDI	dry thickness (nm)	grafting density (nm^{-2})	roughness S_q (nm)
PNIPAAm 42 kDa	w/o C12	42 000	1.2	9.4 ± 0.4	0.18 ± 0.01	0.38
PNIPAAm 94 kDa	w/o C12	94 000	1.2	9.5 ± 0.3	0.08 ± 0.02	0.34
PNIPAAm 104 kDa	w/o C12	104 000	1.3	10.0 ± 0.6	0.08 ± 0.03	0.36
PNIPAAm 105 kDa	w C12	105 000	1.1	7.5 ± 0.3	0.06 ± 0.08	1.31
PNIPAAm 135 kDa	w C12	135 000	1.3	8.5 ± 0.5	0.05 ± 0.07	1.41
PNIPAAm 178 kDa	w C12	178 000	1.1	9.0 ± 0.4	0.04 ± 0.06	1.21
PAA 25 kDa		25 000	1.2	7.0 ± 0.2	0.21 ± 0.09	0.44

Scheme 2. Chemical Structure of the Two PNIPAAm Species Used to Graft As Polymer Brushes: (A) PNIPAAm Synthesized by RAFT Polymerization Which Induces Dodecyl Trithiocarbonate (C12 terminal group) at the End of Each Polymer Chain; (B) PNIPAAm Synthesized by Radical Polymerization; This Polymer Lacks the C12 Terminal Group

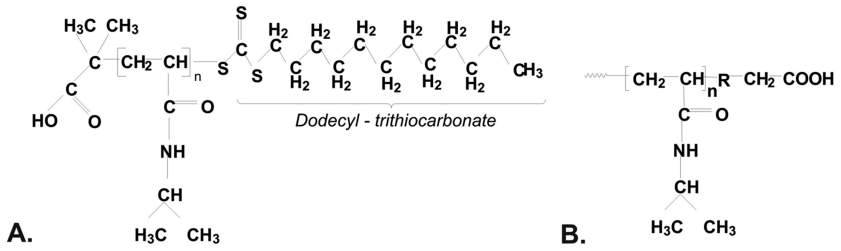

responsive adsorption of water-soluble protein molecules is of great interest for application in biotechnology.

Hence, we investigated the differences in the intrinsic properties and interfacial interactions of brushes made of carboxyl-terminated monoCOOH-PNIPAAm that carries a hydrophobic terminal group (RAFT polymerized) and a monoCOOH-PNIPAAm that lacks this domain (free-radical polymerized). In addition, the adsorption of FGN on homo-PNIPAAm and binary-PNIPAAm-PAA polymer brushes was investigated by means of spectroscopic ellipsometry using physiological salt and pH conditions, at different temperatures, to demonstrate temperature-responsive protein adsorption on the brushes. Scheme 1 illustrates the basic steps of the surface modification with polymer brushes by grafting-to of the binary brush system PNIPAAm-PAA, and the subsequent temperature-responsive protein adsorption with FGN.

2. EXPERIMENTAL SECTION

2.1. Materials. Poly(glycidyl methacrylate) (PGMA), Poly(acrylic acid) (PAA), and two different Poly(*N*-isopropylacrylamide) PNIPAAm species, a reversible addition–fragmentation chain transfer (RAFT) polymerized mono-COOH-PNIPAAm-SC12H_{25}, and a free radical polymerized mono-COOH-PNIPAAm were purchased from Polymer Source, Inc., Canada. The availability of the basic polymers with specified molecular weights for the brush preparation is not always constantly guaranteed. The detailed characteristics about all the polymers used in this work, are listed in Table 1. Ethanol abs. was purchased from VWR, Germany. Chloroform ($CHCl_3$) was purchased from Fisher, Germany. Fibrinogen (FGN) as well as phosphate buffered saline (PBS) buffer (tablets, pH 7.4, 0.01 M) were purchased

DOI: 10.1021/am508161q
ACS Appl. Mater. Interfaces 2015, 7, 12516–12529

Table 2. Properties of the Applied Binary PNIPAAm-PAA Polymer Brushes

binary-brushes	characteristics of PNIPAAm	polymer ratio	dry thickness (nm)	grafting density of PNIPAAm (nm^{-2})	roughness S_q (nm)
PN 42 kDa-PAA	w/o C12	20:80	7.1 ± 0.3	0.03 ± 0.01	0.39
PN 42 kDa-PAA	w/o C12	50:50	8.5 ± 0.7	0.09 ± 0.04	1.68
PN 42 kDa-PAA	w/o C12	80:20	12.5 ± 0.4	0.14 ± 0.02	0.85
PN 105 kDa-PAA	w C12	20:80	8.3 ± 0.5	0,012 ± 0.02	2.91
PN 105 kDa-PAA	w C12	50:50	8.7 ± 0.6	0,050 ± 0.04	2.74
PN 105 kDa-PAA	w C12	80:20	10.3 ± 0.3	0,110 ± 0.01	2.48

from Sigma-Aldrich, Germany. Silicon wafers oriented in [100] direction and with 2 nm native SiO_2 layer from Si-Mat (Landsberg, Germany) or glass slides used in cell culture (VWR, Germany) were used as substrates.

Two different polymerization techniques were used to synthesize the provided linear carboxyl-terminated PNIPAAm polymers: (A) RAFT polymerization, which is a form of free radical polymerization of a substituted monomer in the presence of a suitable chain transfer (RAFT) reagent, and (B) free radical polymerization, by which a successive addition of free radical building blocks forms the polymer.[19,20] Both polymerization procedures lead to the formation of PNIPAAm polymers with low PDI and high functionality. However, PNIPAAm chains produced by RAFT polymerization carry an additional hydrophobic terminal group that consists of a dodecyl trithiocarbonate (C12 terminal group). Scheme 2 shows the chemical structure of the two different PNIPAAm species used in this work in order to graft polymer brushes.

2.2. Preparation of Polymer Brushes. Polymer brushes were prepared by the grafting-to method: Silicon wafers were cut into 1.3 × 2.0 cm^2 pieces, cleaned with ethanol in an ultrasonic bath for 15 min and subsequently activated in an oxygen-plasma chamber for 1 min at 100 W. PGMA solution (0.02 wt % in chloroform) was spin-coated and annealed at 100 °C under vacuum for 20 min resulting in a thin reactive layer with epoxy groups for the following "grafting-to" step. A second polymer solution consisting of monocarboxyl-PNIPAAm (1 wt % in chloroform), was spin-coated and annealed overnight at 150 °C under vacuum. The same procedure was followed for both PNIPAAm types (with and without C12 terminal group). The COOH functionalities reacted with the available epoxy groups of the PGMA functionalized forming esters. Nongrafted polymer was removed by stirring in Millipore water for 4 h and drying with N_2 flux after dipping in ethanol solution. For the preparation of binary brushes PNIPAAm was spin-coated and annealed at different time intervals to achieve different grafted amounts of PNIPAAm. Annealing at 150 °C for 5 min resulted in 20% PNIPAAm in the grafted binary brush layer (i.e., 20:80 brush), whereas annealing for 20 min resulted in 50% (i.e., 50:50 brush), and annealing for 6 h resulted in 80% of PNIPAAm (i.e., 80:20 brush). After extraction with water, a PAA polymer solution (1 wt % in ethanol) was spin-coated on top of the PNIPAAm brush layer and was annealed at 80 °C in a vacuum oven for 30 min. The conditions were chosen so that the remaining epoxy groups of the PGMA reacted with only few COOH-groups along the chain of PAA. Nongrafted PAA was removed by extraction in ethanol (stirring for 10 min; twice). Corresponding PAA homopolymer brushes were prepared, following the same procedure, leading to PAA Guiselin brushes, where the polymers are grafted with more than one anchoring point to the surface, making loops and tails.[21] According to Bittrich et al., these layers can be considered as polymer brushes since the anchoring points n are between $1 < n < 2$ and the swelling ratio is comparable to the swelling ratio of a brush made by end-tethered polymers.[22] Table 1 and 2 give a summary of the characteristics of the polymer brushes used in this work. For both PNIPAAm species three different molecular weights were examined. However, mainly the results of two of them were selected and discussed in this paper; the PNIPAAm of 42 kDa without C12 terminal group (PN42), and the PNIPAAm of 105 kDa with C12 terminal group (PN105).

The dry polymer brush layer thickness (nm), listed in Tables 1 and 2 was measured by means of spectroscopic ellipsometry. The brush grafting density was calculated according to $\sigma = d\rho N_A/M_N$, were d is the ellipsometrically obtained layer thickness (nm), ρ is the polymers' bulk density, N_A is the Avogadro's number, and M_N (g/mol) the polymers' molecular weight. Polymer brush surface roughness S_q was individually estimated by AFM height measurements in tapping mode from a 2 μm AFM image.

2.3. Surface Characterization Methods. *Spectroscopic Ellipsometry.* Ellipsometric measurements are sensitive to changes in the polarization state of light reflected from the surface. Upon reflection, the two ellipsometric parameters, tan Ψ (relative amplitude ratio) and Δ (relative phase shift), are recorded.[23] The ellipsometric angles Δ and Ψ are correlated to the corresponding thickness and refractive index of the probed layers through the basic equation of ellipsometry,[23] eq 1

$$\tan(\Psi)\exp(i\Delta) = \frac{R_p}{R_s} = F(\Phi_0, \lambda, N_s, n_0, n_j, k_j, d_j) \quad (1)$$

were R_p and R_s are the complex reflection coefficients for p and s polarized light respectively, which are complex functions of the angle of incidence Φ_0, the wavelength λ, the optical constants N_s and n_0 of the substrate and the ambient respectively, n_j and k_j the refractive index and its imaginary part; extinction coefficient respectively, as well as the layer thickness d_j. On the basis of this equation, the parameters of the layers can be determined by fitting an optical model to the measured Δ and tan Ψ values.

The ellipsometric analysis, used to estimate the thicknesses and refractive indices of all layers, is described elsewhere.[14,24] Shortly, a spectroscopic ellipsometer equipped with a rotating compensator (alpha-SE, Woollam Co., Inc., Lincoln, NE, USA) was used. The ellipsometer records Δ and Ψ, at wavelengths within the visible optical range of 400−800 nm. The angle of incidence Φ_0 was kept constant at 70°, close to the Brewster angle of silicon. All data were acquired and analyzed using Complete EASE software, version 4.46. The in situ measurements for the investigation of polymer brush swelling were performed in 0.01 M PBS buffer at pH 7.4, using a quartz cuvette (TSL Spectrosil, Hellma, Muellheim, Germany). The wafers were kept fixed in the cuvette by a home-built Teflon holder that helped isolate the in situ components from the environment in order to ensure for pH stability and solution purity.

To evaluate the refractive index n, and dry and swollen brush thickness d, we used a multilayer-box model consisting of silicon, silicon dioxide, anchoring layer PGMA, and the polymer brush.[25] The optical dispersion relations for silicon and silicon oxide were taken from the software library and the refractive index of PGMA was set to $n_{PGMA} = 1.525$.[26] The dependence of the refractive index on the wavelength was described by the Cauchy relation: $n(\lambda) = A + B/\lambda^2$. In case of very thin ($d < 10$ nm) dry brush films, the Cauchy parameters A and B were estimated for a 50 nm thick dry polymer layer, and applied as fixed values in the Cauchy relation. The extinction coefficients $k_j(\lambda)$ of PGMA and of the brushes are zero in the measured spectral range.

For the monitoring of the temperature-dependent swelling/deswelling of the polymer brushes, the temperature of the quartz cuvette was adjusted by a home-built heating stage equipped with test-Point software. The actual temperature at the brush surface was thermostatically controlled. Heating and cooling cycles for each sample were performed between 15 and 40 °C with a heating/cooling rate of 0.2 °C s^{-1}.

Adsorption of Fibrinogen. Prior to FGN adsorption, the brush was let to swell in PBS buffer for 10 min. Adsorption of 0.25 mg/mL FGN

DOI: 10.1021/am508161q
ACS Appl. Mater. Interfaces 2015, 7, 12516−12529

solution in PBS was performed for 16 h either at 25 °C or at 37 °C. After thorough washing with PBS buffer, the FGN-modified brushes were fixed at the bottom of a 70° quartz cuvette. The ellipsometric angles tan Ψ and Δ were monitored in situ, and compared to the ones of the swollen brush layer without protein, determined before FGN adsorption. For the case of FGN adsorption at 37 °C, the brush samples were washed with 37 °C warm buffer to avoid altering of the collapsed chain conformation. As for the swelling/deswelling experiments, also during the measurements of the FGN modified brush layers, the temperature was controlled by a home-built heating stage coupled to a thermostat.

To determine the FGN amount adsorbed on the brushes, we used the de Feijter' equation modified by Xue et al.[8,27,28] Here, after FGN adsorption on the polymer brush, two upgrades in the multilayer-box model are considered. First, the polymer brush layer which was initially described by the $d_{swollen}$ and $n_{swollen}$ components, is considered to uptake a small FGN amount, therefore is now represented by the $d_{combined}$ and $n_{combined}$ (denoted as d_{comb} and n_{comb}) parameters. Moreover, an uppermost layer that consists of solely (hydrated) FGN protein molecules is added to the model. The thickness of the additional layer equals the thickness increase after protein adsorption, (i.e., $d_{add} = d_{comb} - d_{swollen}$) and the refractive index n_{comb} is considered to be common to the FGN-brush layer. Hence, the change of molecular concentration in the FGN-brush layer is represented by $n_{comb} - n_{swollen}$ and in the FGN-ambient layer by $n_{comb} - n_{amb}$. The FGN adsorbed amount, or adsorption density in mg/m^2 can be calculated then by the following equation

$$\Gamma_{FGN} = d_{swollen}\left(\frac{n_{comb} - n_{swollen}}{dn/dc}\right) + d_{add}\left(\frac{n_{comb} - n_{amb}}{dn/dc}\right) \quad (2)$$

were dn/dc is the FGN refractive index increment.[23] Typically, n (λ = 632 nm) is chosen for the calculations.

The validity of the model was tested in direct comparison to the modified de Feijter equation based on the effective medium approximation (EMA),[28] and the estimated adsorbed amount Γ_{FGN} was found to be in agreement for both methodologies. A detailed discussion on the modeling approximation of protein adsorption on polymer brushes is given by Bittrich et al.[28]

Streaming Potential Measurement. The surface electrokinetic properties were investigated by streaming potential measurements in order to calculate the zetapotential. A flow cell made of parallel-plate microchannel was designed to perform these measurements. An electrolyte solution was circulated through this channel with steady flow. In our study, two silicon surfaces coated with equal polymer brushes and/or modified brushes were arranged face to face to form this small channel. Two electrodes were applied at the ends of the channel and the voltage difference (ΔU) versus pressure loss was recorded. The resulting potential difference between the two ends of the channel is defined as the streaming potential. The zetapotential as a function of pH was determined using the ElectroKinetic Analyzer (EKA, Anton PAAr GmbH, Graz, Austria).

Dynamic Contact Angle Measurement. Contact angle measurements provide information concerning the surface free energetic state and wettability. The measurements were carried out as dynamic sessile drop experiments employing an OCA40-microgoniometer (Data-Physics Instruments GmbH, Filderstadt, Germany) at relative humidity (50%), at controlled room temperature; T = 23 °C, and additional at 40 °C. The test liquid was freshly deionized water with a surface tension of 72.8 mN/m. The advancing contact angle (θ_A) was evaluated from dynamic dispensing/redispensing measurements with a volume of the sessile drop of 5 to 10 μL and a suspension rate of 0.2 μL/s. Low suspension rates were chosen to ensure proximity of the advancing to the static contact angle, due to a mechanical equilibrium between single measurement steps. Embedded needle measurements (needle in), were performed and the goniometer technique was used by aligning a tangent at the point of contact between solid surface and sessile drop. Temperature sensitive measurements were performed by the use of a temperature stage (DataPhysics Instruments GmbH) in a temperature range of 23 to 42 °C. The calibrated temperature stage was attached to the contact angle device and the temperature was set 15 min prior to each individual measurement, in order to ensure thermal equilibrium. To ensure experimental performance under equilibrated conditions at each temperature, we closed the system by a cover.

Atomic Force Microscopy. All AFM images were taken in the peak force quantitative nanomechanical analysis imaging mode (PFQNM) by a Dimension ICON equipped with a heating stage (Bruker-Nano, USA). For the measurements in air we used silicon nitride sensors SCANASYST-AIR (Bruker, USA) with a nominal spring constant of 0.4 N/m and tip radius of 5 nm, and for measurements in water at room temperature or at 40 °C we used silicon nitride sensors SCANASYST-FLUID+ (Bruker, USA) with a nominal spring constant of 0.7 N/m and a tip radius of 5 nm. The measurements were done in the noncalibrated mode, i.e. the information about the mechanical parameters (we analyzed the E-modulus channel and the adhesion force channel) is qualitative. The estimation of the RMS roughness S_q was done with the help of the software NanoScope Analysis (Bruker-Nano, USA). Investigation of soft materials in liquids is often difficult and can limit the scan-quality.

2.4. Cultivation of Human Mesenchymal Stem Cells. The polymer brush coatings prepared on glass slides were pretreated first with pure phosphate buffered saline (PBS, Sigma-Aldrich, Germany) for 1h and subsequently with cell culture medium containing 10% fetal calf serum for 2 h at 37 °C. Subsequently, each sample was seeded with 5 × 10^4 cells/500 μL of human mesenchymal stem cell (hMSC, kindly provided from Medical Clinic I, Dresden University Hospital "Carl Gustav Carus", Germany) in 24-TCPS-well-plates and incubated for 72 h at 37 °C and 5% CO_2. For all cell culture experiments the media DMEM (high glucose (4.5 g/L), with L-glutamine, PAA, Austria) has been used which was additional supplemented with 10% fetal calf serum (FCS, Biochrom, Germany), 10 U/mL penicillin and 100 μg/mL streptomycin (Biochrom, Germany).

The morphology of all cells was observed by phase contrast microscopy (Zeiss Axiovert 40 CFL, Germany), whereby images have been taken every 24 h as continuous control of the cell culture. Additionally, fluorescence microscopy (Zeiss LSM510 META, Axioskop2 (FS mot), and AxioCam, Germany) were used. Immunofluorescence staining was carried out by means of the dyes DAPI (Invitrogen, Germany) and Phalloidin-AlexaFlour488 (Sigma-Aldrich, Germany). According to the staining protocol; first the culture medium was removed from the samples in the well and washed 3 times with PBS. The cell samples were fixed by adding 3.7% formaldehyde solution for 30 min at room temperature and subsequently blocked with 1%BSA/0.1%TritonX-100/PBS for 30 min. After three times washing with PBS the mixed staining solution of DAPI and Phalloidin-AlexaFlour488 was applied and the samples were incubated for 60 min.

3. RESULTS AND DISCUSSION

Different PNIPAAm polymers were successfully grafted using a PGMA anchoring layer to silicon or glass surfaces generating a polymer brush with end-tethered polymer chains. The following results describe the influence of the hydrophobic terminus dodecyl trithiocarbonate (PNIPAAm w C12) in comparison to PNIPAAm without terminal group (PNIPAAm w/o C12). While PNIPAAm polymers with different molecular weights were investigated, mainly the results of two, the PNIPAAm 42 kDa "w/o C12" and the PNIPAAm 105 kDa′ w C12′, are discussed below. As a subsequent surface modification step, poly(acrylic acid) PAA was spin coated on top of either PNIPAAm with or without C12 terminus in order to graft PNIPAAm-PAA binary brushes with increased complexity and correlated response to pH and thermal external stimuli.

3.1. Surface Characterization of Homo and Binary PNIPAAm Brushes. The following results describe the

DOI: 10.1021/am508161q
ACS Appl. Mater. Interfaces 2015, 7, 12516−12529

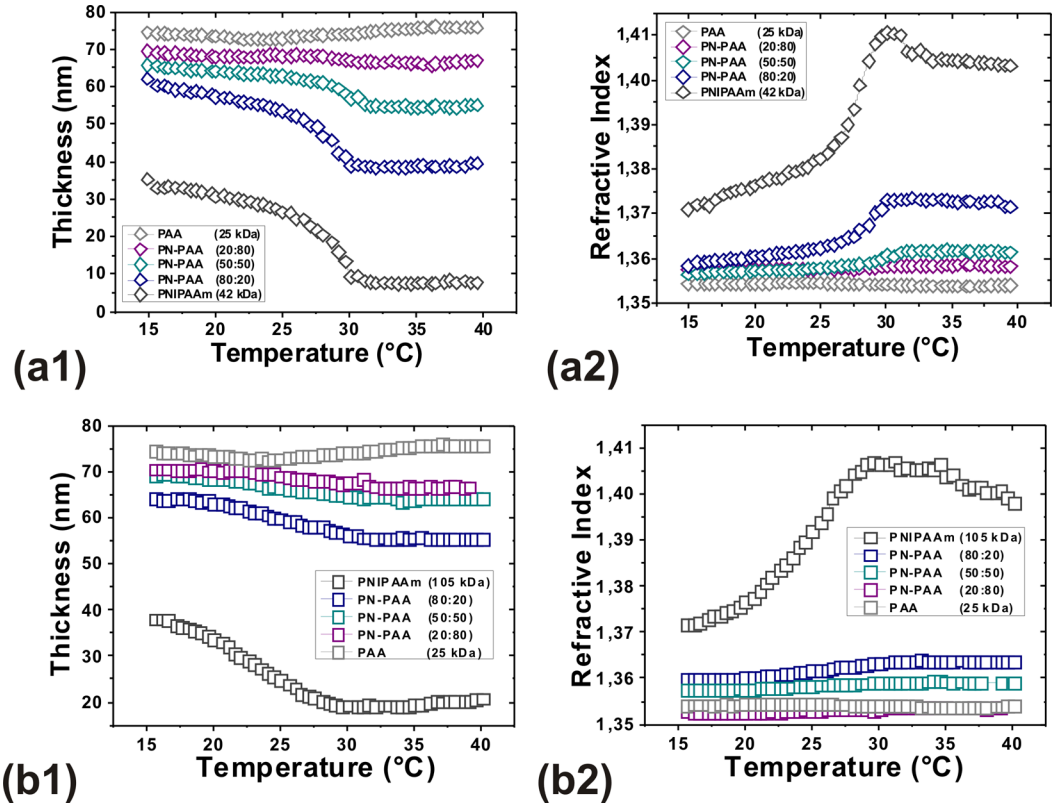

Figure 1. LCST transition of polymer brushes. (a1) Swollen brush thickness and (a2) refractive index of PN42-PAA brushes w/o C12 are compared to (b1) swollen brush thickness and (b2) refractive index of PN105-PAA brushes w C12. The temperature depended swelling was performed in PBS buffer and representative refractive index is shown for λ = 631.5 nm.

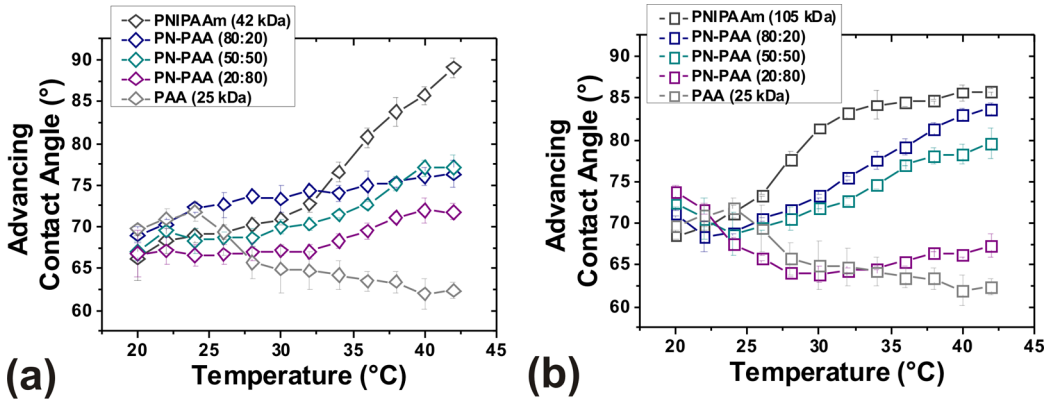

Figure 2. Advancing water contact angle θ_A was measured temperature-dependent: Comparison of PAA homopolymer with PNIPAAm homopolymer and its binary brushes; (a) PNIPAAm 42 kDa, w/o C12, and its binary brushes: PN42-PAA with 20:80, 50:50, 80:20 ratio; (b) PNIPAAm 105 kDa, w C12, and its binary brushes: PN105-PAA with 20:80, 50:50, 80:20 ratio;.

influence of the hydrophobic terminus dodecyl trithiocarbonate (PNIPAAm w C12) in comparison to PNIPAAm without terminal group (PNIPAAm w/o C12).

Figure 1 shows ellipsometric data that relate changes in the swollen brush thickness to the temperature. Plots (a) and (b) compare the temperature sensitive swelling of PNIPAAm brushes w/o and w C12 as well as the complex swelling of the respective PNIPAAm-PAA brushes. On the left, the brush thickness changes are shown (Figure a1, b1) whereas, on the right-hand side the corresponding refractive index values are given (Figure a2, b2), with d and n showing a juxtaposed analogy in every case. In contrast to a sharp LCST transition of PNIPAAm in solution,[29] which occurs within 1 to 2 °C, grafted PNIPAAm exhibits a broader transition due to the confinement in brush geometry and essential inter- and intrachain interactions.[30]

Accordingly, polymer brushes depicted in Figure 1 show a first slow deswelling between 15 and 27 °C, followed by a collapse between 28 and 30 °C. There is a pronounced difference in the LCST behavior between the PNIPAAm brushes w/o C12 (Figure 1, a) and the brushes w C12 terminal group (Figure 1b). That is, the relatively sharp collapse of PNIPAAm chains without C12 between 28 and 30 °C compared to the smooth transition of PNIPAAm chains with C12 in broader temperature range between 15 to 29 °C. In addition, the LCST was found to be 1.0 ± 0.3 °C lower for the

DOI: 10.1021/am508161q
ACS Appl. Mater. Interfaces 2015, 7, 12516−12529

PNIPAAm w C12 ($LCST_{PNIPAAm\_wC12}$ = 29 °C and $LCST_{PNIPAAm\_w/oC12}$ = 30 °C). When the PNIPAAm brushes without C12 surpass the LCST threshold, they show an abrupt reduction of the layer thickness by 10−20 nm. In contrast, brushes of PNIPAAm with the C12 terminal group show a smooth response of the layer thickness to temperature changes. The slope of the curve, which represents the phase transition rate, from 25 to 30 °C is tan θ_{PN42k} = 5.42 for the PNIPAAm w/o C12 and noticeably smaller; tan θ_{PN105k} = 1.33 for the PNIPAAm w C12. Both brush types approach a minimum thickness close to the LCST and then again start slowly to swell, because of thermal motion of the chains.

For PN−PAA binary brushes, a decrease in temperature-sensitive changes of n and d was generally observed with increasing PAA percentage in the layer, as expected. The recorded LCST transition for the PN42-PAA w/o C12 (Figure 1a) was evidently more pronounced in comparison to the binary brushes composed of PNIPAAm w C12 (Figure 1b). In particular, the difference in magnitude of brush layer parameters at low and high temperature was ∼76% for the PN42-PAA 80:20 brush, ∼30% for the PN42-PAA 50:50, and only ∼3% for the PN42-PAA 20:80 brush (w/o C12), whereas for brushes w C12, it was ∼47% for the PN105-PAA 80:20 brush, ∼20% for the PN105-PAA 50:5,0 and ∼13% for the PN105-PAA 20:80 brush (w C12), compared to the n and d change of the according PNIPAAm homo brushes. However, at pH 7.4, a homo-PAA brush shows a thickness increase with increasing temperature (n slightly decreased), because of thermal motion of the PAA chains.

In summary, it was found that the hydrophobic terminus of PNIPAAm led to a broader phase transition, a smaller phase transition rate and a slight decrease of the LCST of the homo brushes. As a component of binary PNIPAAm-PAA brushes, the hydrophobic terminus caused a greater decrease in the temperature sensitivity of the binary brush but a lower dependence on the amount of PAA present in the binary brush.

The surface wettability of homo and binary PNIPAAm polymer brushes without and with hydrophobic functional C12 terminal group are discussed on the basis of conventional dynamic water contact angle measurements in air, with respect to temperature changes from 20 to 44 °C in intervals of 2 °C. In the case of thermoresponsive PNIPAAm homopolymer brushes, the advancing water contact angle increased with the PNIPAAm molecular weight M_n, generally independent of the functional C12 terminus, which is in agreement with previous investigations.[31] However, the brushes made of PNIPAAm w C12 were found to be generally more hydrophobic.

The determined increase in the water contact angle with increasing temperature, shown in Table 3, corresponded to an increased hydrophobic nature of PNIPAAm brushes. The phase transition changes the interfacial wettability due to molecular rearrangements of the polymer brush. Below the LCST the polymer chains strongly interact with water molecules through hydrogen bonding and therefore stretch in solution (i.e., hydrophilic behavior). Above LCST, the formation of hydrogen bonding between water molecules and PNIPAAm chains does not take place, and the brush adopts a collapsed conformation. Hence, the brush layer shows a more hydrophobic character with higher advancing contact angles. Noticeably, this transition is gradual and the dewetting of the polymer chains happens in small increasing ratios as it was previously reported for PNIPAAm thin films.[32] There are some general differences observed between PNIPAAm brushes without and with C12

Table 3. Thermoresponsive PNIPAAm Homopolymer Advancing Water Contact Angles θ_A at the Temperature Range of the Hydration/Dehydration Transition (LCST)

mass (kDa)	θ_A (deg) at 30 °C	θ_A (deg) at 36 °C	LCST transition $\Delta\theta$ (deg)
homo PNIPAAm brush w/o C12			
42	70.9	80.7	9.8
94	75.5	84.0	8.5
104	78.0	85.0	7.0
homo PNIPAAm brush w C12			
105	82.2	84.1	1.9
135	88.9	94.1	5.2
178	92.5	98.4	5.9

(Table 3). Although all PNIPAAm brushes without C12 terminus have sharper LCST transition, defined as delta $\Delta\theta$ in degrees, the PNIPAAm brushes with C12 terminal end group do not show such a fast and pronounced change in $\Delta\theta$. It is interesting to observe that there is a tendency to higher LCST transition values ($\Delta\theta\uparrow$) in dependence on the PNIPAAm molecular weight for PNIPAAm with C12 and in reverse manner ($\Delta\theta\downarrow$) for PNIPAAm without C12. The advancing contact angles of water of the binary PNIPAAm-PAA brushes in dependence on the temperature are shown in Figure 2. As described in the Experimental Section, representative polymer brush samples were chosen. In general, for all binary PNIPAAm-PAA brushes, the advancing water contact angle is lower than for the PNIPAAm homopolymer brushes, which is related to the hydrophilic character of the poly(acrylic acid) PAA component of the mixed brush.[33] Consequently, as higher the PAA fraction of the binary brush, as lower the advancing contact angle of all PNIPAAm-PAA brushes is, independently of the C12 terminus: 20:80 < 50:50 < 80:20. Figure 2 exhibits the wetting behavior of the binary brushes in the investigated temperature range in comparison to the homo PAA and PNIPAAm brushes, respectively. Additionally, an influence of the PNIPAAm C12 terminal group (e.g., 105 kDa) on the wettability was observed. It seems that the C12 terminus had an impact on the polymer chain mobility at the surface. On the one hand, the mixed brushes PN105-PAA (w C12) with the ratios of 80:20 and 50:50 tend to be more hydrophobic than PN42-PAA (w/o C12) brushes with the same ratios. On the other hand, the mixed PN105-PAA brush with 80% poly(acrylic acid) showed a hydrophilicity comparable to the one of the PAA homopolymer brush. In contrast, considering the PN42-PAA 20:80 with high amount of PAA the polymer brush surface is more hydrophobic than the according PN105-PAA 20:80.

One major limitation of the temperature dependent "sessile drop" measurements for these highly water swollen systems is the inaccuracy of the advancing contact angle at high temperatures because of "stick−slip" behavior of the brush at temperatures higher than 28 °C.[34] This phenomenon has been explained by the theory of a "two-component system," which basically implicates a molecular-thermal inhomogeneity in the brush structure.[35] According to the theory, the temperature differences between the very top and the bottom of the brush layer might cause certain changes in motility of polymeric chains, as well as in the dynamics of water and vapor penetration inside the brush. Therefore, we are going to apply in situ captive bubble measurements in future studies, which are further advantageous for the determination of receding contact angles.

DOI: 10.1021/am508161q
ACS Appl. Mater. Interfaces 2015, 7, 12516−12529

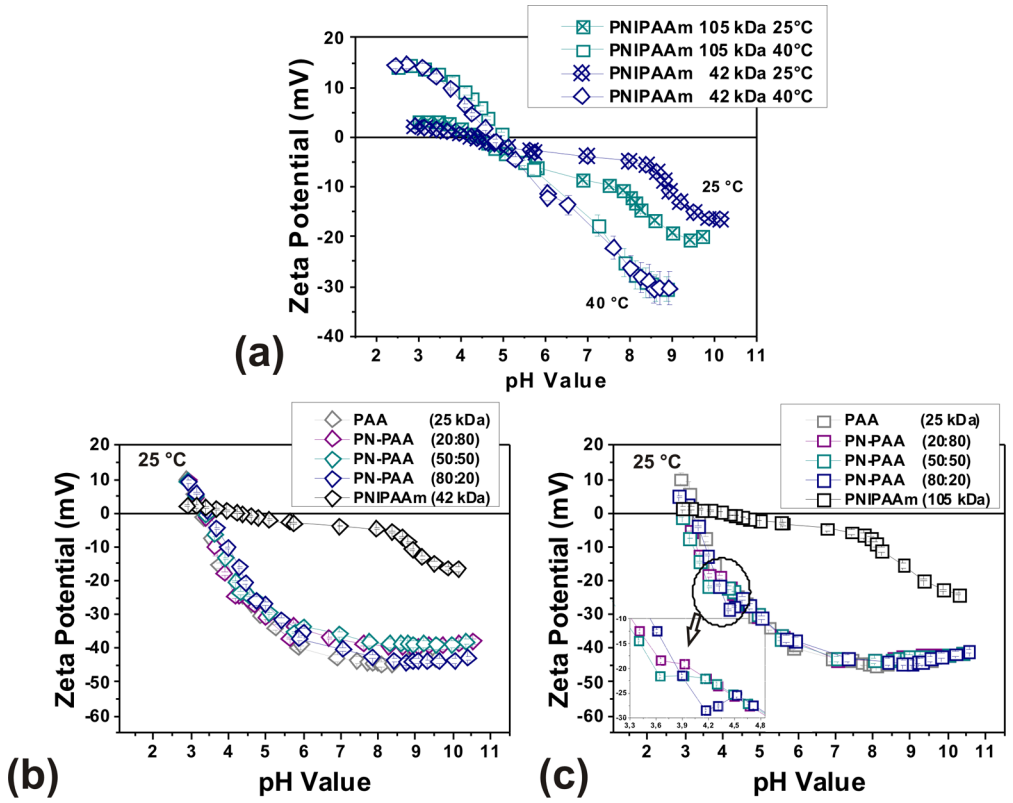

Figure 3. Zeta potential in dependence of pH value, measured in 1×10^{-3} M KCl: (a) thermoresponsive surface behavior of PNIPAAm 42 kDa and PNIPAAm 105 kDa during LCST transition; (b) binary PN42-PAA with different composition; (c) PN105-PAA with different composition.

Summing up, it was found that the hydrophobic terminus C12 of PNIPAAm increased the advancing contact angle quite considerably, and as also observed during the in situ ellipsometry experiments, makes the phase transition less pronounced. Incorporation of PAA in PNIPAAm-PAA binary brushes generally decreases the contact angle, whereasthe presence of the C12 terminus in the mixed brushes leads to higher contact angles for PNIPAAm-PAA brushes with the ratio 80:20 and 50:50 and lower values for the 20:80 brush, compared to the brushes where PNIPAAm had no hydrophobic end. This indicates that at the surface of the binary brushes PNIPAAm w C12 is more present for smaller amounts of PAA and less when the brush contains 80% PAA compared to the brushes containing PNIPAAm w/o C12.

Streaming potential measurements were performed in order to understand the electrokinetic surface properties of the homo and binary brushes. Figure 3 combines three graphics showing the comparison between PNIPAAm without C12 terminal group (42 kDa) and PNIPAAm with C12 terminal group (105 kDa) and their binary PNIPAAm-PAA brushes.

All PNIPAAm homopolymer brushes, independently on the C12 terminal group and molecular weight M_n (Table 1), have an isoelectric point around pH_{IEP} 4.2 at 25 °C. The zeta-potential values vary in dependence on the pH because of the charge formation process due to ion adsorption at the interface, typically for surfaces that do not have dissociable groups. In this process, the alteration of the absolute zeta potential value with pH is caused by the preferential adsorption of hydroxide or chloride ions (OH^- or Cl^-) at pH > IEP and hydronium ions or cations (H_3O^+) at pH < IEP, from the electrolyte. As an example, numerous studies revealed that hydrophobic materials possess a negative surface charge in neutral and alkaline solutions and isoelectric points close to pH 4.[36,37] Especially, for the charging of water/hydrophobic wall interfaces, the hydroxide ion adsorption was found to dominate over the adsorption of hydronium ions at neutral and alkaline pH. At pH values below 4, hydronium ions adsorption is dominating.[38] The flat zeta potential curves for both PNIPAAm homopolymer brushes 42 kDa and 105 kDa indicate similar highly swollen brush surfaces without dissociable groups; (Figure 3a black symbols). The high degree of swelling was also confirmed by ellipsometric measurements. There is a direct influence of the swelling process of a thin polymer layer on the electrokinetic properties. The uptake of high water content can be considered as a process competing ion adsorption. To that effect, several studies proved that a layer of strongly oriented water molecules is formed at hydrophobic solid surfaces and that this interfacial water structure—and thus the hydroxide ion adsorption—is modulated by the hydration of the electrolyte ions.[38] According to Kanamaru et al. the zeta potential of swollen surfaces decreases with increasing adsorption of water because the ions in the double layer are replaced by water molecules.[35]

In summary, the zeta-potential curves of PNIPAAm w and w/o C12 above the LCST did not differ (Figure 3a). Below the LCST higher zeta-potential values were found for pH > pH_{IEP}, which indicates less swelling of PNIPAAm w C12 brushes. In contrast to Synytska et al.,[39] the zeta potential curves of the PNIPAAm homopolymer brushes were not linear in this pH range. The curves show a bend around pH 8, which could be due to surface heterogeneities or polymer structure rearrangements. As described before, at hydrophobic surfaces (formed above the LCST) the hydroxide ion adsorption is preferred and hence the absolute zeta potential values increase. In the

DOI: 10.1021/am508161q
ACS Appl. Mater. Interfaces 2015, 7, 12516−12529

collapsed conformation of the brush where the polymer chains are dehydrated, there might be less structural rearrangements possible, which is the reason the bend in the zeta potential curve disappeared. However, the discussion of the course of the zeta potential curves is generally difficult and indirectly related to the position of the shear plane which is changing with swelling−deswelling processes.

Figure 3b describes the zeta potential function of binary PN42-PAA (w/o C12) and Figure 3c of binary PN105-PAA (w C12) both with different amounts of PAA. It can be easily seen that the negatively charged polyelectrolyte poly(acrylic acid) is dominant at the surface because the zeta potential curves of all binary PNIPAAm-PAA brushes resemble with the zeta potential curve of the PAA homo brush. The zeta potential function of the PAA brush (25 kDa, gray symbol) is typical for a surface with dissociable functional carboxylic groups which has a plateau range from pH values higher than 7, where the carboxylic groups are completely dissociated. The isoelectric points either of the PAA homo brush or binary PN42-PAA (w/o C12) and PN105 PAA (w C12) brushes are similar and have a value of pH 3.2. There is only one irregularity to observe in case of the binary PN105-PAA brushes carrying the C12 terminus. There is a bend in the zeta potential curve in the lower pH region between pH 3 and 5 where the carboxylic groups are not, or are incompletely dissociated (Figure 3c, inset). As long as the carboxylic groups are dissociated they tend to determine the surface properties of the binary polymer brushes. However, there could be interfacial hydrophobic interactions caused by the alkyl chains of the terminal group C12, which may cause structural rearrangements in the double layer of the surface. It is assumed that the bend illustrates changes in the charge formation process and is more pronounced in the zeta potential function the higher the contents of PNIPAAm 105 kDa in the binary polymer brush. In summary, it has to be stated that PAA was found to dominate the surface properties of the investigated binary brushes completely, independent of the presence of the hydrophobic terminus C12. Surface morphology, elasticity (E-modulus), and adhesion force were examined by atomic force microscopy measurements. Among the PNIPAAm homopolymer brushes, brushes of PNIPAAm with C12 terminus have a higher roughness in contrast to the ones without C12 (Table 1). This increased roughness was also found for the binary brushes made out of PNIPAAm 105 kDa w C12 (Table 2 and 4). Figure 4 shows AFM images of the homo polymers PAA and both PNIPAAm species as well as their resultant binary brushes. The illustrated E-modulus is only qualitatively determined. All measurements were done under the same conditions, which means that antilever spring constant, tip radius and sensitivity were the same for all AFM-experiments. The color of the skin of the AFM images in Figure 4 shows qualitative differences of the E-modulus. The E-modulus is larger the brighter the image appears. Brighter features were measured for both the PNIPAAm homopolymer 105 kDa with C12 terminus and its binary brushes PN105-PAA with ratios 20:80 and 80:20. PNIPAAm 105 kDa w C12 seems to dominate the surface. In addition, the surface shows homogeneously distributed structured areas with distinct brightness which can be explained as different elasticity or stiffness. However, the pronounced topography with higher roughness (Table 4) influences also the E-modulus. In case of PNIPAAm 42 kDa homopolymer without C12 terminus the surface has a lower E-modulus similar to the PAA homopolymer brush. With respect to the binary brushes PN42-PAA, the E-modulus depends on the amount of the PNIPAAm in the brush. The lower the amount of PNIPAAm 42 kDa, the lower the the E-modulus of the polymer brush: 20:80 < 80:20.

Figure 4. AFM images (3D topography; skin in color of elasticity—brighter = higher E-modulus) of homo PNIPAAm polymer brushes (left) and binary PNIPAAm-PAA brushes out of them (right), measured at room temperature and at air. All AFM-images have an equal size: 500 nm × 500 nm; *z*-scale is 20 nm.

Table 4. Comparing the Roughness S_q of Binary PNIPAAm Brushes, Measured in Dry State and in Wet State under Distilled Water at Room Temperature 23°C, and at Elevated Temperature 40°C

binary polymer brushes	dry roughness S_q (nm), T = 23 °C	roughness S_q (nm), under water, T = 23 °C	roughness S_q (nm), under water, T = 40 °C
PN42-PAA 20:80	0.39	3.22	4.21
PN42-PAA 80:20	0.85	2.44	0.91
PN105-PAA 20:80	2.91	3.88	4.36
PN105-PAA 80:20	2.48	4.19	1.67

DOI: 10.1021/am508161q
ACS Appl. Mater. Interfaces 2015, 7, 12516−12529

Further in situ AFM experiments focused on binary brushes PN42-PAA and PN105-PAA stored under distilled water at 23 and 40 °C in order to investigate the response of the surface characteristics according the LCST transition (Figure 6). From Table 4 it can be seen, that the surface roughness is mainly influenced by the PAA content of the brushes. Regarding the roughness data, there is no effect of the C12 terminus and also the influence of the different conformation of PNIPAAm above and below the LCST is less than the impact of the PAA content. This is an additional hint to a dominating influence of PAA on the in situ surface properties of binary brushes.

Studying the adhesion force of binary brushes qualitatively in situ, Figure 5 shows that there are distinguished areas with

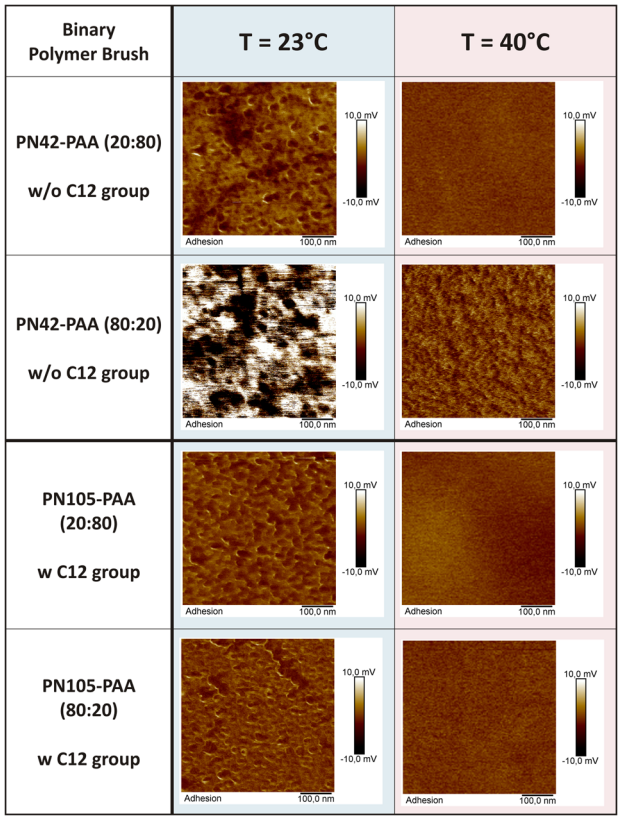

Figure 5. 2D AFM images (adhesion force, qualitatively): comparison of the adhesion force of binary PNIPAAm brushes, swollen in water at 23 °C, and at elevated temperature 40 °C.

different adhesion forces in case of all binary brushes at 23 °C. Also here, the brighter features demonstrate the structures with more pronounced adhesion force. After increasing the temperature to 40 °C the distribution of adhesion force is homogeneous over the whole AFM image.

In summary from the AFM investigations can be concluded that the C12 residue causes a higher E-modulus of PNIPAAm homopolymer brushes and thereby a lesser elasticity compare to PNIPAAm brushes without C12 terminus. This dominant effect is also transferred to the binary PNIPAAm brushes with C12 in dry state (Figure 4, right). For swollen binary brushes, it is observed, that the PAA brush component is dominating the surface properties. This is even more pronounced above the LCST when the PNIPAAm chains are collapsed (more homogeneous 2D AFM images in Figure 5, right).

3.2. Fibrinogen Adsorption on PNIPAAm Polymer Brushes. The adsorption of fibrinogen (FGN) was investigated on homo- and binary brushes, with and without C12 terminal group, at two different temperatures; below the LCST at 25 °C, and above LCST at 37 °C, and the results are shown in Figure 6. The analysis was performed via visible spectroscopic ellipsometry, and the changes in the ellipsometric angles as directly estimated dynamic data, sensitive to any small surface state variations, were recorded. The net absolute variations of the ellipsometric angles, before and after protein (FGN) adsorption on the surface, are translated into thickness and refractive index correlated changes, and can be further equated to quantitative values of protein amount adsorbed on the surface (Γ_{FGN} mg/m^2) as described above.[8] The ellipsometric measurements have been performed in situ, in a controlled temperature environment, at physiological conditions (PBS buffer, pH 7.4, 0.01 M) and the initial FGN concentration was 0.25 mg/mL.

Figure 6a shows the FGN adsorption on the less hydrophobic brushes which did not contain the C12 terminal group; whereas Figure 6b refers to the results of FGN adsorption on C12 containing brushes. Both graphs show similar trends, with a higher adsorbed amount for all cases of C12 containing brushes, indicating the prospective increase in hydrophobic interactions between the brush and the protein molecules. Moreover, the preserved protein repellent character of PNIPAAm above LCST vanishes when the hydrophobic segment C12 is introduced into the brush. At 37 °C the collapsed PNIPAAm 105 kDa brush clearly alters affinity toward FGN and an increase in protein adsorption is observed.

For the PAA homobrush, only a very small amount of FGN protein adsorbed at room temperature, and almost no FGN was found to adsorb at 37 °C. Adsorption on the "wrong site" of the electrostatics, where both surface and protein are negatively charged, is generally small. The buffer salt concentration (137 mM [Na^+] in PBS) does not seem to suppress electrostatic repulsion between brush and FGN completely. At higher temperatures, the increase in thermal motion of the polymer chains as well as the higher rate of FGN Brownian motion in solution prevents almost entirely any protein adsorption. Introduction of a small amount of PNIPAAm (PNIPAAm-PAA 20:80 and 50:50) into a binary brush leads to an increase of the adsorbed amount with increasing content of PNIPAAm. The effect of temperature on protein adsorption is small, at T = 37 °C less protein is adsorbed. The reason for this may be that at this temperature, the PNIPAAm chains are collapsed and the electrostatic repulsion of FGN by the PAA chains becomes more noticeable. A completely different behavior was found for the brushes containing only 20% of PAA. Here the adsorbed FGN amount increased considerably at T = 37 °C. A very high difference of the adsorbed amount at $T < T_{LCST}$ and $T > T_{LCST}$ was found for the brush containing PNIPAAm w C12.

It seems that at the interface of a brush of this composition PAA is no longer able to influence the surface properties, even when PNIPAAm is collapsed. The brushes PNIPAAm-PAA (80:20) were proven to have the highest temperature sensitivity of the tested binary brushes (compare Figure 1). Therefore, the chain conformation of PNIPAAm should have a major impact on the ability of these binary brushes to adsorb proteins. In the collapsed state, PNIPAAm is more hydrophobic and therefore more likely to adsorb proteins. The temperature sensitivity was found to be higher for binary brushes containing PNIPAAm w/

DOI: 10.1021/am508161q
ACS Appl. Mater. Interfaces 2015, 7, 12516−12529

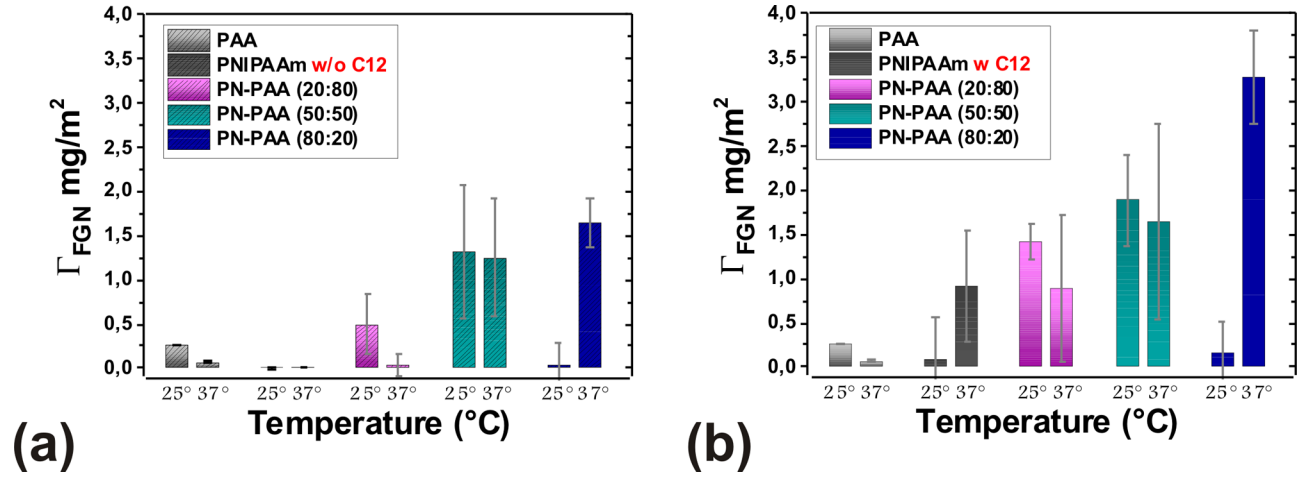

Figure 6. Adsorbed amount of FGN protein on homo- and binary polymer brushes, (a) without C12 and (b) with C12. The experiments were performed under physiological conditions pH 7.4.

o C12, nevertheless the temperature effect on protein adsorption was much bigger for the brush containing the hydrophobic residue. That means that the hydrophobic nature of the brush overcompensates the lower temperature sensitivity.

PNIPAAm w/o C12 homo brushes were found to be protein repellent below and above the LCST. PNIPAAm w C12 brushes lose their protein repellence above the LCST. Binary brushes containing also PAA show a complex swelling behavior because between the two components of the brush hydrogen (H) bonds are formed when the carboxylic group of PAA is protonated.[22] Because the FGN adsorption experiments were carried out at pH 7.4, PAA is supposed to be completely deprotonated (compare Figure 3), the chains are stretched and the swelling of PNIPAAm is not hindered (compare Figure 1).

It seems that the ratio of the components forming the binary brushes is crucial for protein adsorption on those brushes: until an amount of 50% PAA in the brush, the adsorbed amount of FGN can be decreased by applying a Temperature $T > T_{LCST}$, whereas in brushes containing only 20% PAA, PNIPAAm is dominating the temperature sensitive behavior, which leads to an increased protein adsorption at $T > T_{LCST}$. This effect is considerably amplified by introducing a hydrophobic terminal residue to PNIPAAm, which may be due to the increased hydrophobic character of PNIPAAm w C12 brushes, but also to an increased flexibility of the chains.

3.3. Cell Adhesion on Homo and Binary PNIPAAm Brushes. Preliminary experiments have shown that the applied parameters of the grafting-to method (includes, e.g., annealing, ethanol extraction, organic solvents) are able to provide sterile polymer brush substrates directly. Therefore, all polymer brush samples were used straightforward for cell adhesion tests without any further sterilization process. This has the advantage that the polymer brush surface structure will be preserved and no damage will occur, a well-known problem of sterilization techniques. Comprehensive practical cell adhesion studies regarding the influence of cell culture medium (DMEM, RPMI-1640), the cell density, the percentage of fetal calf serum in the medium and the need of the time-dependent preincubation in buffer solution (data not shown) led us to the results discussed beneath. In the present paper, we focused on the correlation between both the molecular weight of different PNIPAAm polymers grafted to glass substrates and the different chemical termination of PNIPAAm (i.e., w C12 or w/o C12) with cell adhesion/detachment behavior. For this purpose, we used human mesenchymal stem cells (hMSC) cultivated with same cell density on all different homo PNIPAAm polymer brushes described in Table 1. In general, all investigated homo PNIPAAm brushes formed rapidly cell spheroids (cell aggregates) independent of the molecular weight and the terminal group of the PNIPAAm polymer within 24 h, while on the TCPS control a cell monolayer was formed. The typical size of the hMSC spheroids ranged between 50 to 100 μm. After 72 h of cultivation almost all cell spheroids were detached from each PNIPAAm brush surface and stayed like under floating conditions. By means of UptiBlue assay and LDH assay the viability maintenance of the cells in the spheroids were monitored and proved (data not shown).

Apparently, the diameter of hMSC spheroids is considerable smaller (even single hMSC were observed) on homo PNIPAAm brushes carrying the hydrophobic terminal group C 12 (spheroids <30 μm). Exemplary, Figure 7 exhibits two representative molecular weights, each of the different PNIPAAm polymer species cultivated with hMSC for 72 h. It

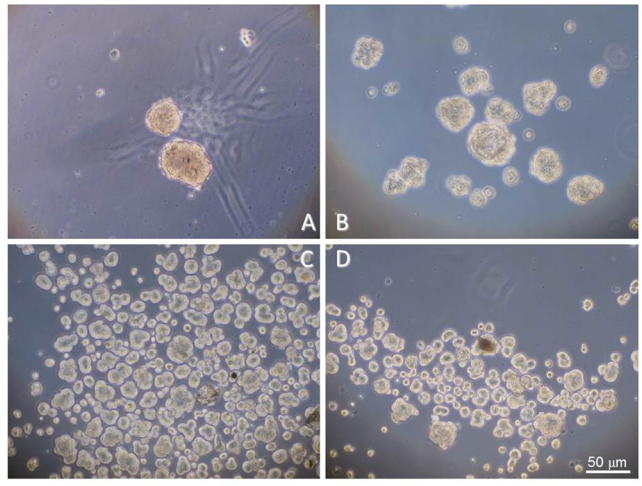

Figure 7. Formation of hMSC spheroids after 72 h of cultivation on different homo PNIPAAm brushes: (A) PNIPAAM 42 kDa (w/o C12), (B) PNIPAAm 94 kDa (w/o C12), (C) PNIPAAm 135 kDa (w C12), (D) PNIPAAm 178 kDa (w C12).

DOI: 10.1021/am508161q
ACS Appl. Mater. Interfaces 2015, 7, 12516−12529

is clearly observed that the altered surface properties of homo PNIPAAm brushes with C12 terminus influence the cell adhesion behavior.

Although the impact of the modified hydrophobicity, elasticity, and chemical heterogeneity on the cell adhesion was evident regarding the C12 terminus of PNIPAAm, the influence of the molecular weight was not so clearly indicated. Especially in the case of homo PNIPAAm brushes without hydrophobic terminal function, no molecular weight effect on cell spheroid formation and its size was found. However, homo PNIPAAm polymer brushes with C12 terminus tend to cultivate slightly bigger cell spheroids using lower molecular weight PNIPAAm polymers compared to higher M_n-PNIPAAm. The results of FGN adsorption have shown that the protein is attracted by PNIPAAm with C12 terminus particularly at 37 °C, i.e. above the LCST. Due to these findings, the increased protein adsorption is also an indication for the differences of the cell response. The known hydration/dehydration transition of PNIPAAm was definitely modified by the C12 terminus, what the described cell culture experiments could also reflect.

Additionally, the binary polymer brushes consisting of the polyelectrolyte PAA and one of the PNIPAAm species described in Table 2 were investigated. First, in contrast to the homo PNIPAAm brushes, hMSCs were forming a monolayer on the homo PAA brush similar to the TCPS control (well plate). Accordingly, in case of all binary polymer brushes, which were composed of PAA and one PNIPAAm species in different ratio, monolayers were formed. There was no difference in the cell response between PN105-PAA (image not shown) and PN42-PAA brushes. It was to observe that as higher the content of the PAA component in the polymer brush was, as better was the monolayer formation. In Figure 8, hMSC cell adhesion after 72 h cultivation on the PAA brush, the TCPS control, and one example of binary PNIPAAm(42 kDa)-PAA brush with a ratio of (20:80) is represented.

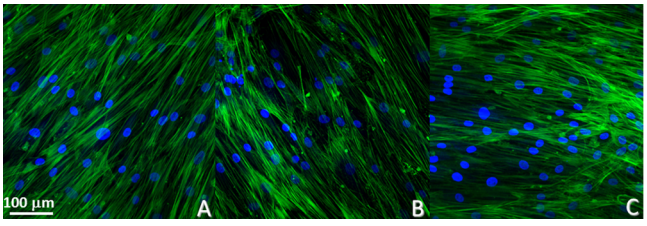

Figure 8. Fluorescence microscopy images of hMSCs after staining with DAPI (blue, nucleus) and with Phalloidin (green, F-actin): (A) homo PAA(25 kDaA) brush; (B) TCPS control; (C) binary PNIPAAm-PAA brush (20:80).

Although a lower content of PNIPAAm (20%) caused a well-formed cell monolayer a higher amount of PNIPAAm (>80%; data not shown) could show the tendency of hMSC aggregation. It was clearly indicated that higher ratios of PAA suppressed the 3D cell culture spheroid formation. In summary, not any of the binary polymer brush samples formed 3D cell spheroids in the same morphology as the PNIPAAm homopolymer brushes during the 72 h. From our studies, we assumed that the protein adsorption capability of the compared polymer brushes and their elasticity could be the key parameters of 3D cell spheroids formation or the cell behavior in general.

4. CONCLUSION

The interfacial characteristics of variable PNIPAAm polymer brushes grafted to silica surfaces were investigated in situ by means of visible spectroscopic ellipsometry (vis-SE), atomic force microscopy (AFM), streaming potential measurements as well as by dynamic contact angle measurements. Two different PNIPAAm species were grafted to the surface in order to prepare homopolymer brushes: the first PNIPAAm polymer possessed the hydrophobic dodecyl-terminal function (C12 terminus), whereas the other PNIPAAm polymer had no such group. Binary brushes were made using one species of both PNIPAAm types, and the polyelectrolyte PAA in different compositions. The intention of the study was to investigate the influence of the terminal hydrophobic group of PNIPAAm on physicochemical surface characteristics, protein adsorption and cell adhesion on homo and binary brushes. It was shown that the hydrophobic terminus lead to a more hydrophobic wetting behavior, decreased temperature sensitivity, broader phase transition, and higher E-modulus of the PNIPAAm homo brushes. In PNIPAAm-PAA binary brushes, PAA was found to dominate the surface properties. PNIPAAm w C12 as a component of binary brushes decreased the temperature sensitivity and increased the hydrophobicity and the E-modulus of those brushes. Protein adsorption experiments were performed at temperatures below and above the LCST using FGN as a model protein. It was found that PNIPAAm w C12 homo brushes lose their protein repellence above the LCST (in contrast to brushes w/o C12). Binary brushes containing also PAA show a complex behavior at which the ratio of both components is crucial for protein adsorption on those brushes: until an amount of 50% PAA in the brush the adsorbed amount of FGN can be decreased by applying a temperature $T > T_{LCST}$, whereas in brushes containing only 20% PAA, PNIPAAm dominates the temperature-sensitive behavior, which leads to an increased protein adsorption at $T > T_{LCST}$. This effect is considerably amplified by introducing a hydrophobic terminal residue to PNIPAAm, which may be due to the increased hydrophobic character of PNIPAAm w C12 brushes. In hMSC cell adhesion experiments, it was observed that at all investigated PNIPAAm homo polymer brushes 3D cell spheroids were rapidly formed. When PNIPAAm w C12 was present, the size of the hMSC cell spheroids decreased. Binary PNIPAAm-PAA brushes, however, formed hMSC monolayers caused by the PAA component of the binary system.

It has to be stated that binary brushes made from PAA and PNIPAAm are highly promising to control and modulate the interaction with biomolecules. We have proven several leverages (as composition, molecular weight, chemical modification of a brush component) to tailor the response of biomolecules to such a brush, but there are many more, as, i.e., grafting density, use of specific terminal groups, that can be used to tailor such systems. However, it has also to be concluded that from in situ surface characterization results as, for example, zeta-potential curves, it cannot be directly concluded how a biomolecule will behave on strongly swollen flexible thin films like polymer brushes. In summary, grafted-to homo and binary PNIPAAm polymer brushes are highly promising surface coatings with switchable, stimuli responsive interaction characteristics, capable of accommodating a variety of biotechnological related applications.

DOI: 10.1021/am508161q
ACS Appl. Mater. Interfaces 2015, 7, 12516−12529

AUTHOR INFORMATION

Corresponding Authors

*E-mail: uhlmannp@ipfdd.de.

*E-mail: koenig-ulla@ipfdd.de.

Author Contributions

†E.P. and U.K. contributed equally to this work.

Notes

The authors declare no competing financial interest.

ACKNOWLEDGMENTS

This work was primarily supported by the German Science Foundation (DFG) within the projects DFG-Nr. STA 324/49-1 and EI 317, in the context of the "Materials World Network". We express our sincere thanks to Prof. Dr. Manfred Stamm for the pleasant and enriching discussions and his manifold support. The authors thank Anja Caspari for the introduction to and performance of streaming potential measurements. In addition, we thank Carolin Böhm, who prepared the polymer brush samples and performed dynamic contact angle measurements.

REFERENCES

(1) Ayres, N. Polymer brushes: Applications in Biomaterials and Nanotechnology. *Polym. Chem.* **2010**, *1*, 769−777.

(2) Hoy, O.; Zdyrko, B.; Lupitskyy, R.; Sheparovych, R.; Aulich, D.; Wang, J.; Bittrich, E.; Eichhorn, K. J.; Uhlmann, P.; Hinrichs, K.; Müller, M.; Stamm, M.; Minko, S.; Luzinov, I. Synthetic Hydrophilic Materials with Tunable Strength and a Range of Hydrophobic Interactions. *Adv. Funct. Mater.* **2010**, *20*, 2240−2247.

(3) Motornov, M.; Roiter, Y.; Tokarev, I.; Minko, S. Stimuli-Responsive Nanoparticles, Nanogels and Capsules for Integrated Multifunctional Intelligent Systems. *Prog. Polym. Sci.* **2010**, *35*, 174−211.

(4) Brittain, W. J.; Minko, S. *A Structural Definition of Polymer Brushes. J. Polym. Sci., Part A: Polym. Chem.* **2007**, *45*, 3505−3512.

(5) Stuart, M. A. C.; Huck, W. T. S.; Genzer, J.; Müller, M.; Ober, C.; Stamm, M.; Sukhorukov, G. B.; Szleifer, I.; Tsukruk, V. V.; Urban, M.; Winnik, F.; Zauscher, S.; Luzinov, I.; Minko, S. Emerging Applications of Stimuli-Responsive Polymer Materials. *Nat. Mater.* **2010**, *9*, 101−113.

(6) Quinn, A.; Mantz, H.; Jacobs, K.; Bellion, M.; Santen, L. Protein Adsorption Kinetics in Different Surface Potentials. *Europhys. Lett.* **2008**, *81*, 1−6.

(7) Uhlmann, P.; Houbenov, N.; Brenner, N.; Grundke, K.; Burkert, S.; Stamm, M. In-Situ Investigation of the Adsorption of Globular Model Proteins on Stimuli-Responsive Binary Polyelectrolyte Brushes. *Langmuir* **2007**, *23*, 57−64.

(8) Xue, C.; Yonet-Tanyeri, N.; Brouette, N.; Sferrazza, M.; Braun, P. V.; Leckband, D. E. Protein Adsorption on Poly (N -isopropylacrylamide) Brushes: Dependence on Grafting Density and Chain Collapse. *Langmuir* **2011**, *27*, 8810−8818.

(9) Burkert, S.; Bittrich, E.; Kuntzsch, M.; Müller, M.; Eichhorn, K. J.; Bellmann, C.; Uhlmann, P.; Stamm, M. Protein Resistance of PNIPAAm Brushes: Application to Switchable Protein Adsorption. *Langmuir* **2010**, *26*, 1786−1795.

(10) Xue, C.; Choi, B. C.; Choi, S.; Braun, P. V.; Leckband, D. E. Protein Adsorption Modes Determine Reversible Cell Attachment on Poly(N-isopropyl acrylamide) Brushes. *Adv. Funct. Mater.* **2012**, *11*, 2394−2401.

(11) Balamurugan, S.; Mendez, S.; Balamurugan, S. S.; Ii, M. J. O. B.; Lo, G. P. Thermal Response of Poly (N -isopropylacrylamide) Brushes Probed by Surface Plasmon Resonance. *Langmuir* **2003**, *19*, 2545−2549.

(12) Wu, J. Y.; Liu, S. Q.; Heng, P. W. S.; Yang, Y. Y. Evaluating Proteins Release from, and their Interactions with, Thermosensitive Poly (N-isopropylacrylamide) Hydrogels. *J. Controllled Release* **2005**, *102*, 361−72.

(13) Yu, Q.; Zhang, Y.; Chen, H.; Zhou, F.; Wu, Z.; Huang, H.; Brash, J. L. Protein Adsorption and Cell Adhesion/Detachment Behavior on Dual-Responsive Silicon Surfaces Modified with Poly(N-isopropylacrylamide)-Block-Polystyrene Copolymer. *Langmuir* **2010**, *26*, 8582−8588.

(14) Bittrich, E.; Burkert, S.; Mu, M.; Eichhorn, K.- J.; Stamm, M.; Uhlmann, P. Temperature-Sensitive Swelling of Poly(N -isopropylacrylamide) Brushes with Low Molecular Weight and Grafting Density. *Langmuir* **2012**, *48*, 1606−16015.

(15) Becker, A. L.; Henzler, K.; Welsch, N.; Ballauff, M.; Borisov, O. Proteins and Polyelectrolytes: A Charged Relationship. *Curr. Opin. Colloid Interface Sci.* **2012**, *17*, 90−96.

(16) Tsapikouni, T. S.; Missirlis, Y. F. pH and Ionic Strength Effect on Single Fibrinogen Molecule Adsorption on Mica Studied with AFM. *Colloids Surf., B* **2007**, *57*, 89−96.

(17) Zhao, T.; Chen, H.; Zheng, J.; Yu, Q.; Wu, Z.; Yuan, L. Inhibition of Protein Adsorption and Cell Adhesion on PNIPAAm-Grafted Polyurethane Surface: Effect of Graft Molecular Weight. *Colloids Surf., B* **2011**, *85*, 26−31.

(18) Yu, Q.; Zhang, Y.; Chen, H.; Wu, Z.; Huang, H.; Cheng, C. Protein Adsorption on Poly(N-isopropylacrylamide)-Modified Silicon Surfaces: Effects of Grafted Layer Thickness and Protein Size. *Colloids Surf., B* **2010**, *76*, 468−474.

(19) Li, J.; Chen, X.; Chang, Y. Preparation of End-Grafted Polymer Brushes by Nitroxide-Mediated Free Radical Polymerization of Vaporized Vinyl Monomers. *Langmuir* **2005**, *16*, 9562−9567.

(20) Yang, Y.; Song, X.; Yuan, L.; Li, M.; Liu, J.; Ji, R.; Zhao, H. Synthesis of PNIPAM Polymer Brushes on Reduced Graphene Oxide Based on Click Chemistry and RAFT Polymerization. *J. Polym. Sci., Part A: Polym. Chem.* **2012**, *50*, 329−337.

(21) Aubouy, M.; Guiselin, O.; Raphae, E. Scaling Description of Polymer Interfaces: Flat Layers. *Macromolecules* **1996**, *29*, 7261−7268.

(22) Bittrich, E.; Kuntzsch, M.; Eichhorn, K. J.; Uhlmann, P. Complex pH- and Temperature-Sensitive Swelling Behavior of Mixed Polymer Brushes. *J. Polym. Sci., Part B: Polym. Phys.* **2010**, *48*, 1606−1615.

(23) Werner, C.; Eichhorn, K. J.; Grundke, K.; Simon, F.; Grählert, W.; Jacobasch, H. J. Insights on Structural Variations of Protein Adsorption Layers on Hydrophobic Fluorohydrocarbon Polymers Gained by Spectroscopic Ellipsometry (Part I). *Colloids Surf., A* **1999**, *156*, 3−17.

(24) Bittrich, E.; Rodenhausen, K. B.; Eichhorn, K. J.; Hofmann, T.; Schubert, M.; Stamm, M.; Uhlmann, P. Protein Adsorption on and Swelling of Polyelectrolyte Brushes: A Simultaneous Ellipsometry-Quartz Crystal Microbalance Study. *Biointerphases* **2010**, *5*, 159−67.

(25) Höök, F.; Vörös, J.; Rodahl, M.; Kurrat, R.; Böni, P.; Ramsden, J. J.; Textor, M.; Spencer, N. D.; Tengvall, P.; Gold, J.; Kasemo, B. A Comparative Study of Protein Adsorption on Titanium Oxide Surfaces Using In Situ Ellipsometry, Optical Waveguide Lightmode Spectroscopy, and Quartz Crystal Microbalance/Dissipation. *Colloids Surf., B* **2002**, *24*, 155−170.

(26) Van Krevelen, D. W.; Te Nijenhuis, K. In *Properties of Polymers: Their Correlation with Chemical Structure; Their Numerical Estimation and Prediction from Additive Group Contributions*; Elsevier: Amsterdam, 1992; Chapter 4, pp 97−98.

(27) De Feijter, J. A.; Benjamins, J.; Veer, F. A. Ellipsometry as a Tool to Study the Adsorption Behavior of Synthetic and Biopolymers at the Air-Water Interface. *Biopolymers* **1978**, *17*, 1759−1772.

(28) Hinrichs, K.; Eichhorn, K. J. In *Ellipsometry of Functional Organic Surfaces and Films*; Springer: Berlin, 2014; Chapter 5, pp 79−105.

(29) Li, W.; Wu, P. On the Thermodynamic Phase Behavior of Poly(N-vinylcaprolactam) Solution in the Presence of Different Ionic Liquids. *Polym. Chem.* **2014**, *5*, 761−766.

(30) Zhulina, E. B.; Borisov, O. V.; Pryamitsyn, V. A.; Birshtein, T. M. Coil-Globule Type Transitions in Polymers. 1. Collapse of Layers of Grafted Polymer Chains. *Macromolecules* **1991**, *24*, 140−149.

DOI: 10.1021/am508161q
ACS Appl. Mater. Interfaces 2015, 7, 12516−12529

(31) Takei, Y. G.; Aoki, T.; Sanui, K.; Ogata, N.; Sakurai, Y.; Okano, T. Dynamic Contact Angle Measurement of Temperature-Responsive Surface Properties for Poly(N-isopropylacrylamide) Grafted Surfaces. *Macromolecules* **1994**, *27*, 6163−6166.
(32) Cordeiro, A. L.; Zimmermann, R.; Gramm, S.; Nitschke, M.; Janke, A.; Schäfer, N.; Grundke, K.; Werner, C. Temperature Dependent Physicochemical Properties of Poly(N-isopropylacrylamide-co-N-(1-phenylethyl) acrylamide) Thin Films. *Soft Matter* **2009**, *5*, 1367−1377.
(33) Houbenov, N.; Minko, S.; Stamm, M. Mixed Polyelectrolyte Brush from Oppositely Charged Polymers for Switching of Surface Charge and Composition in Aqueous Environment. *Macromolecules* **2003**, *36*, 5897−5901.
(34) Wan, L.; Meng, X.; Yang, Y.; Tian, J.; Xu, Z. Thermo-Responsive Stick-Slip Behavior of Advancing Water Contact Angle on the Surfaces of Poly(N-isopropylacrylamide)-Grafted Polypropylene Membranes. *Sci. China: Chem.* **2010**, *53*, 183−189.
(35) Kisou, B. Kanamarou. Rheological Treatment of the Rate of Setting of Adhesive Joints. *Colloid Polym. Sci.* **1963**, *192*, 51−66.
(36) Schweiss, R.; Welzel, P. B.; Werner, C.; Knoll, W. Dissociation of Surface Functional Groups and Preferential Adsorption of Ions on Self-Assembled Monolayers Assessed by Streaming Potential and Streaming Current Measurements. *Langmuir* **2001**, *17*, 4304−4311.
(37) Zimmermann, R.; Dukhin, S.; Werner, C. Electrokinetic Measurements Reveal Interfacial Charge at Polymer Films Caused by Simple Electrolyte Ions. *J. Phys. Chem. B* **2001**, *105*, 8544−8549.
(38) Zimmermann, R.; Rein, N.; Werner, C. Water Ion Adsorption Dominates Charging at Nonpolar Polymer Surfaces in Multivalent Electrolytes. *Phys. Chem. Chem. Phys.* **2009**, *11*, 4360−4364.
(39) Synytska, A.; Svetushkina, E.; Puretskiy, N.; Stoychev, G.; Berger, S.; Ionov, L.; Bellmann, C.; Eichhorn, K. J.; Stamm, M. Biocompatible Polymeric Materials with Switchable Adhesion Properties. *Soft Matter* **2010**, *6*, 5907−5914.

DOI: 10.1021/am508161q
ACS Appl. Mater. Interfaces 2015, 7, 12516−12529